ISSN 1330-3651 (Print), ISSN 1848-6339 (Online) https://doi.org/10.17559/TV-20220711123816
Original scientific paper

Structural Investigation of a Historical Masonry Arch Bridge under Far-Fault Earthquakes

Memduh KARALAR*, Mustafa YEŞIL

Abstract: In this research, it is aimed to observe a feature study around the assessment of static and dynamic productivity of a historical arch bridge (HAB) (Konjic Bridge (KB)) in view of dissimilar far fault earthquakes (FFEs). To explore the conduct of FFEs on KB, finite element model (F-E-M) of the KB is assembled and evaluated under various FFEs using ANSYS. Then, FFEs are considered as a result of their distinct, destructive velocity pulse characteristics. The maximum displacement values were found and correlated with the principal stresses and strains. At the conclusion of this investigation, it is observed that the arch of HAB has not more impact on the structural reaction of HAB. Furthermore, it is obviously detected that tensile stresses have not got the critic tensile strength (TS). Additionally, life cycle assessment (LCA) for HAB is also explored and observed that improving the longtime stress/strain values for HAB reduces the HAB life-expectancy dramatically.

Keywords: ANSYS; far fault ground motions; finite element method; masonry arch bridge

1 INTRODUCTION

For historical masonry constructions like bridge containing several structural parts such as quarry stone work, keystone, pavement, etc., it could be very significant to study the effect of FFEs. This effect could be a leading focus mostly for the character of assembly conjunction with the reagent of acceleration, velocity, displacements, stress dispersion etc. [1-6]. It is usually accepted that resonance properties and spectral response generally perform together with structure altitude especially for conventional constructions rather than multipart structure [7, 8]. Because of this reason, the seismic effects which are cited above still involve to be more investigated for the complex constructions such as HAB. Moreover, acceleration, velocity, displacements, stress dispersion etc. due to the multipart masonry assemblies similarly converted a significant subject in the properties of soil structure relations [9-17]. During the past, human existences built bridges in various dissimilar approaches and procedures, from the unassuming approaches to the recent technology, and removed distinctive mechanisms. In HABs, the arch method was generally chosen. In the previous stages where today's manufacturing abilities and building resources are not presented, it is probable to permit great spans or transfer heavy weight charges with the arch system which is unique for the simple essentials of the HAB. Arch bridges, which are frequently realized in Turkey, were constructed by the Ottomans in the arrangement of a stone arch system, especially in the 19th century. These ancient structures, which extend to the present and have a history of thousands of years, have been destroyed or damaged due to various tragedies that have occurred in some periods. At the present time, an unusual consideration is needed to surviving state way and rail systems. Currently, the majority of bridges in the path system as well as conventional bridges in the European rail system involve these masonry bridge constructions, in addition to the extraordinary need for the survival of the state path and rail systems [18]. Because of the importance of HAB constructions, in the literature there are several analytical and experimental researches on the masonry constructions such as buildings, old bridges, etc. [19-27]. At the side of these studies, Özmen and Sayın observed the influence of SSI on a single-span HAB via non-linear time-history analysis [28]. At the end of this study, Özmen and Sayın found that the CS and TS of the stone were not an overpass for the fix base, while for the SSI, the TS of the stone was the overpass [28]. The additional research is made by Hatzigeorgiou et al. Hatzigeorgiou et al. created a model of HAB using F-E-M and conducted linear and non-linear studies on the model [29]. In the other investigation carried out by Fanning and Boothby, the Griffith bridge in Dublin, Ireland, has been investigated using ANSYS software as 3-D solid components, and Fanning and Boothby have completed an investigation of the models [30]. Fanning and Boothby described the consequences of field analysis and FE displaying three HABs [30]. Bridges are verified with a reference frame built under the bridge structure. The LVDT is mounted on the reference structure to measure physical movements, and the structure is loaded with a tool of defined loads. Non-linear F-E-Ms are investigated with ANSYS. It is initiated that 3D non-linear F-E-M with an allowable set of substantial belongings aid good estimate of the genuine productivity of a MAB. Frunzio et al. have carried out another research [31]. Frunzio et al. have carried out 3D F-E-M of a stone MAB [31]. While this model includes non-linear material productivity, it also initiates this analysis highly dependent on the precision of mechanical parameters, frequently problematic to assess with experimental analysis, especially in the case of older constructions. Another research is completed by Toker and Unay. In this study, the exact displaying methods were similarly considered on a sample model of an extensive arch bridge under altered predication situations [32]. Ural showed the dynamic features of Cosandere HAB with SAP2000 [33]. Ural also performed an earthquake investigation of the arch bridge [33]. The other investigation is achieved by Bayraktar et al. Bayraktar et al. investigated the active features of Historical Sinik Bridge, and similarly restructured the bridge F-E-M by regulating the border form definitions [34]. The additional research is done by Brencich and Sabia. In this study, Tanaro Bridge was investigated [35]. In this research, the ordinary frequencies, mode forms and damping percentages of these 18 spans of HAB are investigated by dynamic examinations. Diamanti et al. investigated non-destructive ground-penetrating radar (GPR) on HAB for observing ring separation [36]. To approve and inform of the analytical consequences, numerous experiment site trials were performed. Additional research is done by Aydın and Özkaya. In this study, it was similarly considered the failure loads of HAB, and a research was completed targeting the computation of

the performances of the single-spanned HABs demonstrations under definite loads using the method of static investigation [37]. Bouzas et al. conducted an investigation on the effect of the distribution of the thickness sizes of the arches on the load bearing capability evaluation of a historical stone bridge in Galicia, Spain [38]. At the end of this investigation, Bouzas et al. achieved numerous reliability-based structural assessments of the same bridge [38]. In another investigation, Alpaslan et al. estimated load-carrying ability and carried out consistency examination of a current HAB via the response surface-based F-E-M calibration method to existent crucial situations for the ability assessments of other related MABs [39]. At the end of this investigation, the perpendicular load-carrying ability of MABs with the aid of non-linear methods was obtained, and the non-linear load-carrying ability was chosen in the assessment examination of the bridge. In conclusion, rate proportions demonstrating the real productivity of the bridge were gotten. The other study was carried out by Şeker and Sahin. In this study, Şeker and Sahin examined the seismic performance of the Uşak Clandras Bridge via linear and non-linear time history analysis [55]. At the end of this investigation, Şeker and Sahin found that the compressive stress rate is 6 times bigger than the tensile stress rate [55]. Damages are determined at the ends of the infill wall. Batar et al. offered an influential, confidential, and quick multidisciplinary method for the analysis of HABs [56]. For this aim, Terrestrial laser scanning (TLS) was chosen to define the bridge geometry with high accuracy. At the end of the study, Batar et al. offers very quick and extremely precise information for defining the structural geometry that will offer the essential investigation [56]. As mentioned above, only rare researches offered nowadays concern themselves with the seismic assessment of HAB. The aim of this investigation is to consider the productivity of HAB under FFEs through F-E-M and to establish the ability and productivity estimating. For this aim, the seismic activity productivities of KB built in Bosnia and Herzegovina are explored. First, the features and geometric belongings of the HAB are considered, and the improving of the original FE models is then defined associated with the original estimates of bridge features. Additionally, LCA for HAB under this strong motion is also explored. Detailed discussion of the KB is offered in the following sections.

2 DEPICTION OF THE HAB (KB)

The HAB (KB) considered in this investigation is a beautiful example of 17th century classical Ottoman architecture. On the bridge with 6 arches of pointed form, the arch openings are 6.72 m with 13.56 m among. The length of the two wing walls is 86.20 m and the outside of the railings is 5.35 m. The arches are built on five pieces of masonry built on stone pendants with dimensions of 5×12 meters on wooden beams consisting of 2 and 3 rows. The height of the inscription pavilion is 16.27 m. While the history of the bridge is examined, it is detected that the bridge has been serving safely for many years. It is known to be intact and usable for nearly 263 years, until 1945, while it was severely damaged during World War II. As a result of the bombing in the last days of World War II, which caused the destruction of many historical buildings throughout the world, the bridge was heavily damaged and the four arches of the bridge were completely destroyed as presented in Fig. 1.

Figure 1 The collapse of the KB during World War II (1945) [40]

In order to connect the two sides, the remaining arches of the bridge were demolished and a wooden construction bridge was formed. For the reuse of the bridge, the parts just above the stirrup line were completely demolished, and the cones in the heel and nose sections were completely removed. Subsequent concrete head and reinforced concrete pavement caused serious damage to the bridge legs. The pointed nose on the upstream side was damaged by the debris coming from the floods. As a result of the changes in the river bed and sand and gravel removal from the river on the upstream side, carvings have been formed in the footsteps of the bridge and decay and breaks have occurred in the flexible energy-damping wooden grids among the ground and the bridge. As a result of lack of care, vegetation on the stone surfaces and consequent floral degradation occurred. The original stone and mortar samples of the bridge were examined and the properties of the mortar mixtures and stones to be used in the restoration were determined. The application project was developed according to these data by examining the original stones extracted from the water belonging to the destroyed parts of the bridge and the photographs and engravings showing the original state of the HAB are as presented in Fig. 2.

(a)

(b)

(c)

Figure 2 KB: a) bridge Arch Completed on a Pier; b) completed Bridge Arches; c) general view [40]

3 MODELING OF THE HAB

The FE model of the HAB is made and investigated in several FFEs with the program ANSYS [41]. Information of the F-E-M is presented in the following parts.

3.1 Component Forms

In the F-E-M of HAB, the assembly is separated into minor and modest components related by interconnecting nodes with grades of independence suitable to the part kind

designated for demonstrating the assembly performance in several predication situations. The HAB is shown with 10-node high-order tetrahedron elements. This component has quadratic transposition productivity and is fine matched for exhibiting irregular meshes and contact surfaces [42]. Therefore, such a component is appropriate for estimating the external contact among HAB constituents and the unequal geometry of the F-E-M. Each nodule of the component has three degrees of independence. The interaction procedure of the F-E-M needs the description of interaction exteriors. Information of the interaction exterior forming is specified in the next division.

3.2 Contact Modeling

Interaction process is the work of the distortion produced via hard forms which contact parts at single or extra facts [42]. In this research, the interaction among the HAB and then their modules is distinct as an external-to-external interaction form in which the interaction part might possibly alternate as a role of the grade of departure of the interaction faces. The interaction form is recognized while an exterior of one form comes from interaction with the exterior of additional form and it is usually practiced for random forms that have huge interaction parts [43, 44]. To describe an interaction external couple, one of the externals is selected as an interaction part and added as target part. Both components require the equal specific constraints such as amount of nodes, node places etc. [43]. For the interaction edge of the HAB, CONTA174 section and a similar TARGE170 section are selected to characterize interaction besides departure among the two appearances [44, 45] as presented in Fig. 3. Therefore, bonded interaction is selected among the HAB and their modules.

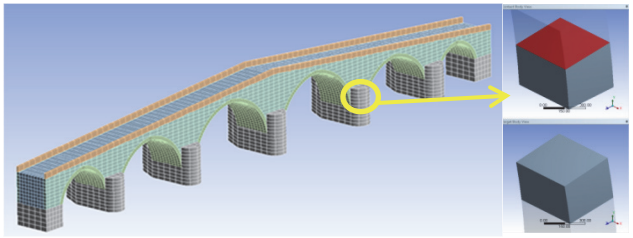

Figure 3 Parts of interaction exteriors [27]

3.3 Mesh System

Dimension and form in mesh system are significant to exactly guess the stress and/or strain worth in F-E-M. Therefore, to declare a suitable mesh system thickness in the F-E-M of the HAB, case studies with altered mesh dimensions are accepted. Consequently, four meshing possibilities are tried and related in the F-E-M. These meshes are offered in Fig. 4. The first alternative is an automatically-produced mesh and it contains 65545 components and 525952 nodes. Another alternative, Tetrahedrons mesh involves 215464 elements and 647894 nodes. The belongings of the additional alternatives are presented in Tab. 1. In F-E-M, larger quantities of nodes cause unnecessary calculation. Thus, the Tetrahedrons meshing choice is selected since the attained mesh has a good dimension delivery through the F-E-M and reduced quantity of nodes. Formerly, the designated meshing alternative is confirmed with several mesh dimensions beginning with 250 mm (the length is 250 mm, adjusts to width perpendicular to length) and decreasing the mesh dimension till the consequences convert to unchanging. The biggest mesh length giving constant consequences is then selected for the F-E-M. Accordingly, the mesh proportions are contributed by hand and engaged as 25 mm inside the contact sections and 50 mm inside the rest of the HAB.

Table 1 Sums of mesh properties in place of dissimilar mesh method

Number#	Mesh Form	Nodes	Elements
Number #1	Automatic	374474	26590
Number #2	Hex Dominant	525952	65545
Number #3	Sweep	374474	26590
Number #4	Tetrahedrons	647894	215464

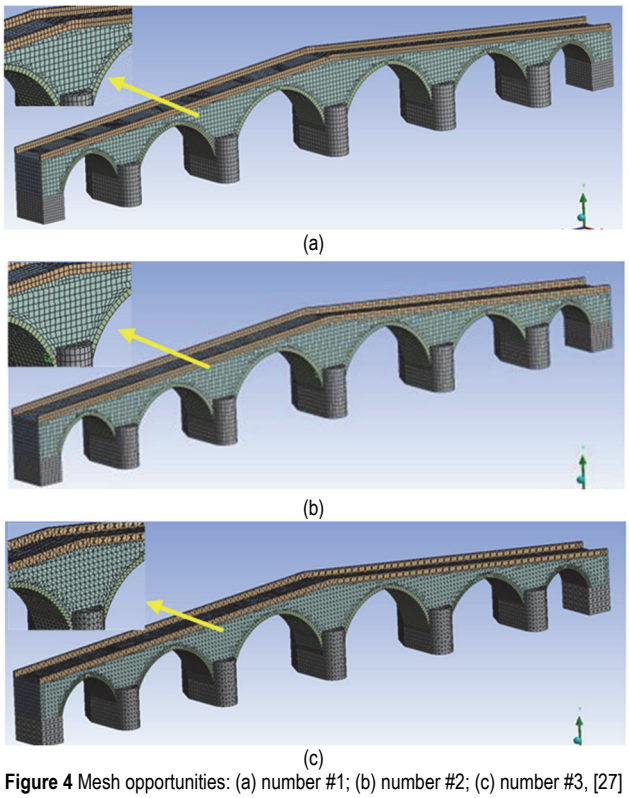

(a)

(b)

(c)

Figure 4 Mesh opportunities: (a) number #1; (b) number #2; (c) number #3, [27]

3.4 Solid Model and Border Conditions

In the non-linear F-E-M, definite solid belongings of the HAB are required to realize accurate research consequences. The resources belongings used in the studies are offered in Tab. 2 [35].

Table 2 Supplies properties [32]

Material	Modulus of elasticity / N/m^2	Poisson ratio	Density / kg/m^3
Stone arches	3.0×10^9	0.25	1600
Timber block	1.5×10^9	0.05	1300
Side walls	2.5×10^9	0.20	1400

Exact description of the border situations is of countless significance in the F-E-M and, subject on the assembly, can significantly affect the productivity. The border situations are described via fixing the translational and revolving amounts of choice at all HAB. All points of freedom of the regions are controlled in all directions [54].

Boundary situations are designated as constant translational and rotating grades of freedom for all historical masonry bridge piers.

4 DISTANT FAULT GROUND MOVEMENTS

FFEs are deliberated as a result of their distinct, damaging velocity pulse features. Tab. 3 shows the FFEs used in this investigation. This group of seismic activity records used in the studies covers an extensive variety of FFEs parameters as presented in Fig. 5.

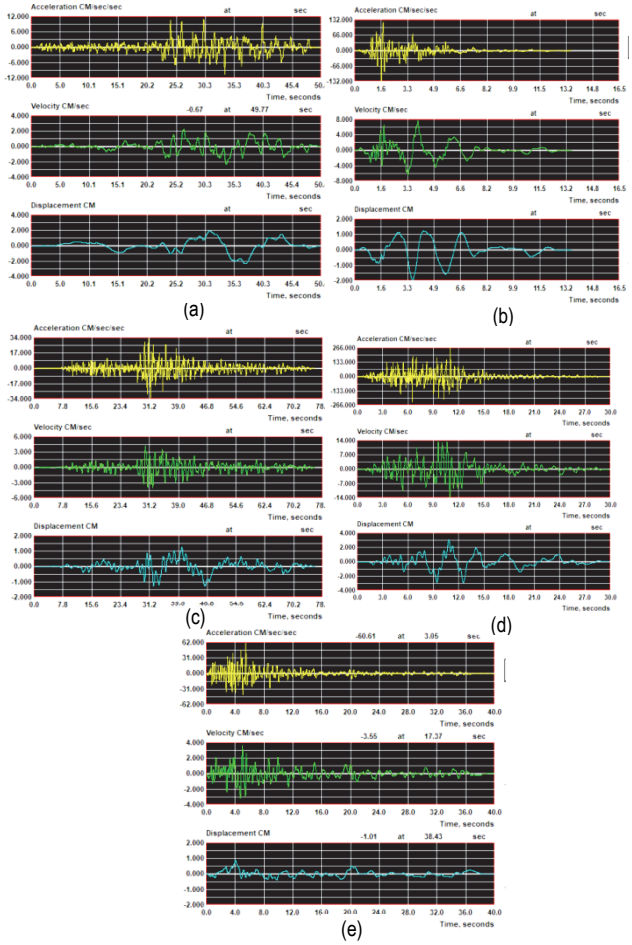

Figure 5 Far fault eartquakes: (a) EQ #1; (b) EQ #2; (c) EQ #3; (d) EQ #4; (e) EQ #5

The size (V_p) and period (T_p) of the velocity pulse are often used to describe FFEs. Nevertheless, the latest investigation by Makris and Black mentions that peak ground acceleration (A_p) is a supplementary important factor to describe the FFEs [44]. Therefore, both A_p and V_p that are contained including the A_p/V_p percentage of strong motion are chosen to define the FFEs reflected in this investigational study. A_p/V_p percentage is similarly illustrative of the main frequency and energy substance of the FFEs [8]. Although strong motion with short-duration acceleration pulses is accompanied by high A_p/V_p percentages, low A_p/V_p percentages indicate strong motion with intense, continuous acceleration pulses. One set of these is selected. This contains a set of 5 earthquakes with A_p/V_p proportions alternating among 4.7 s^{-1} and 23.6 s^{-1} offered in Tab. 3.

Table 3 The FFEs used in this study

#	EQ.	Station/ Component	A_p	V_p	A_p/V_p
			g	cm/s	s^{-1}
1	Borrego Mount,1968	Hollywood Storage Lot / 180°	0.01	2.33	4.7
2	Friuli, Italy, 1976	Conegliano / 0°	0.03	4.29	7.7
3	Kobe, 1995	FUK / 0°	0.05	3.52	13.6
4	Morgan Hill, 1984	San Fran. Int. Airport/ 90°	0.06	3.65	16.7
5	NW California, 1941	Ferndale City Hall / 45°	0.02	0.76	23.6

5 ANALYSES OF CONSEQUENCES

In this section, the conduct of KB under FFEs is explored. For this aim, as mentioned above, FFEs with forward rupture directivity effect are observed attributable to their distinct, destructive velocity pulse appearances. Before the dynamic analysis, it is explored static conduct of KB under ordinary gravitation as presented in Fig. 6.

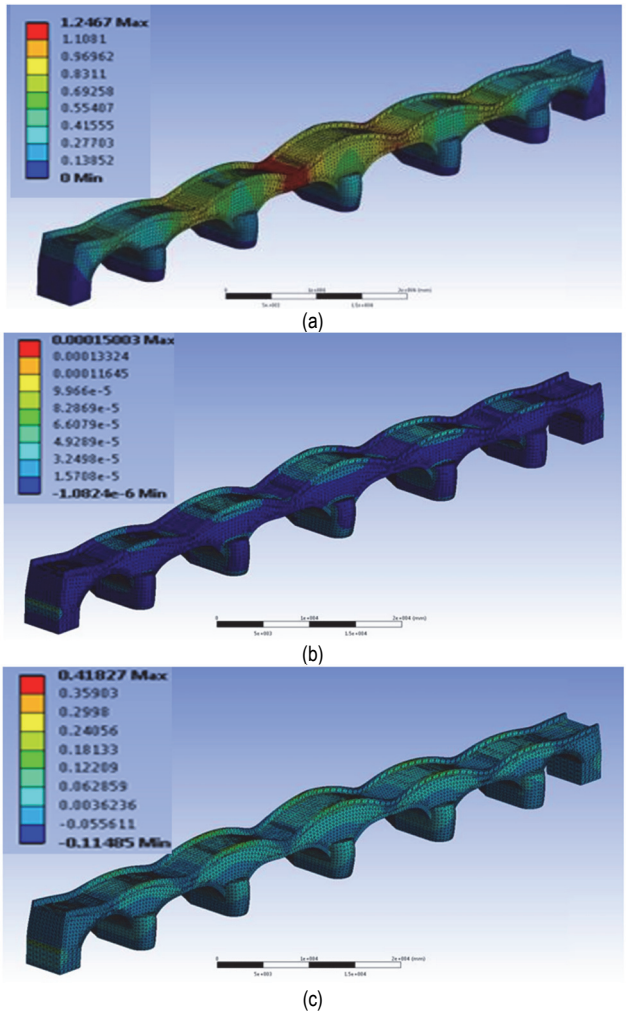

Figure 6 (a) HAB Ordinary gravitation; (b) HAB max. principal as under ordinary gravitation; (c) max. principal stress

As observed in Fig. 6, it is observed that Elastic strain and Max. Principal Stress values are so small values. Observing the analyses consequences under ordinary gravitation, it appears that stress and displacement values did not result in the failure of the KB. As a result of the analyses made, it is observed that the KB can confidently

carry the stresses that occur under its own weight. In addition, while the consequences of the analysis are inspected, it is observed that the loads taking place in the middle part of the KB are determined at the archway ends, causing the maximum stresses to occur in these parts. Stress and displacements diagrams are obtained as presented in Fig. 7 and Fig. 8. Supposing the KB is steady and undamaged below ordinary gravitation, it might be supposed that there will be no destruction to the KB with the TS improved up to 0.47 MPa. It might be supposed that this TS found is according to the TS/compressive strength (CS) percentages (1/20 -1/10) suggested by Pela et al. for masonry constructions and that might be used as a control in evaluating the destruction possible [18]. As a result, as indicated above, in this point, the TS/CS percentage is gauged as 1/20 or 5% and the possible destruction is calculated. So, it is estimated that the values showing the TS larger than 1/20 or 5% might be decreased damage in the HAB. Additionally, examining Fig. 7 and Fig. 8, it has been found that the tension, which indicates the tensile values by the FFEs, is extra important especially along the wide belt. As observed from Fig. 8, the TS was obtained between 0.43 MPa - 0.47 MPa as a consequence of the FFEs and it was observed that it was not beyond the TS of the KB recognized as 1MPa. Once the F-E-M is considered in part it is detected that the TS at 647894 nodes is not bigger than 1 MPa. These conclusions showed that damage may not be formed by TS in FFEs. As the pressure stresses under FFEs are relatively smaller than the CS of KB, no destruction is predictable as a result of pressure. Fig. 7 and Fig. 8 display that the stress showing tensile value on the KB surface under FFEs is not more than 1 MPa which may not be dangerous in terms of destruction. As can be observed from Fig. 7 and Fig. 8, the high edge of the archway, the lowest edge, and the outside of the trail might be suggested as serious for destruction. These consequences are in relation to the consequences in the researches touching their individual weightiness and seismic activity capacity. In the next phases, ruptures that may happen beneath accumulative load consequences might be predictable to onset from these sections and influence the failure mechanism. Dynamics analyses consequences are offered in Tab. 4.

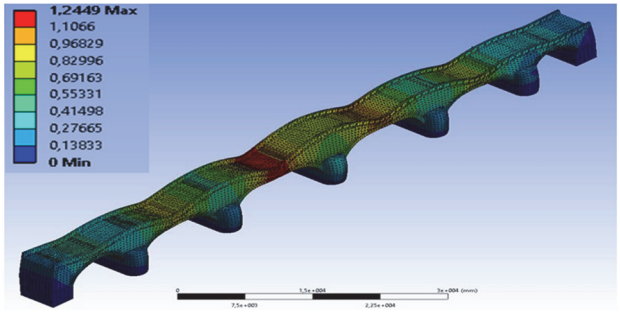

(a)

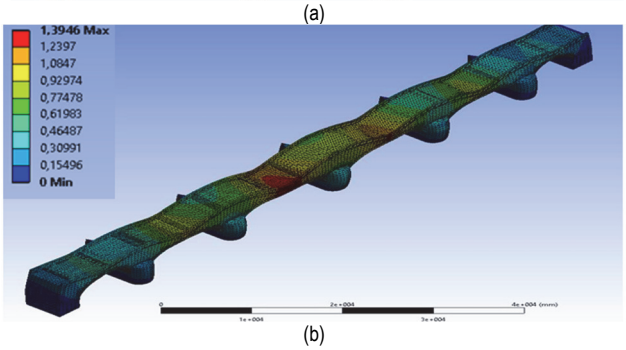

(b)

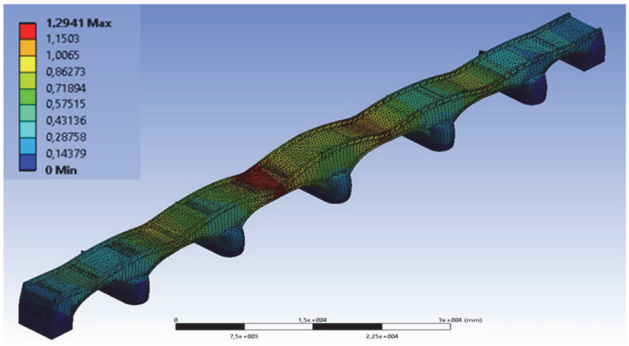

(c)

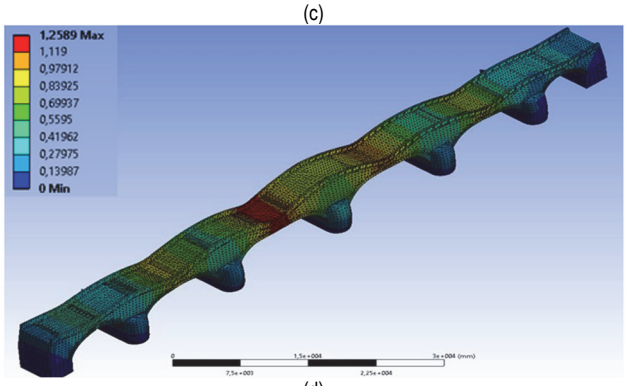

(d)

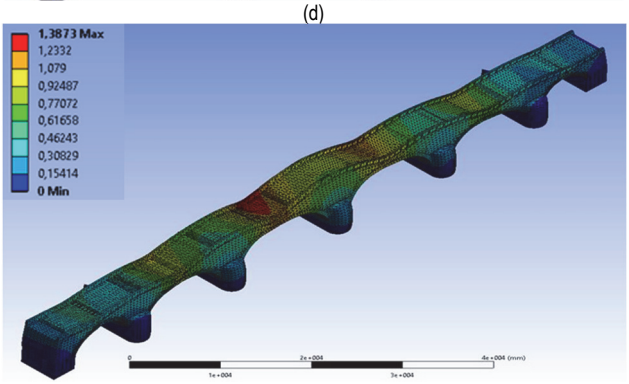

(e)

Figure 7 HAB displacements under far fault earthquakes: (a) EQ. #1; (b) EQ. #2; (c) EQ. #3; (d) EQ. #4; (e) EQ. #5

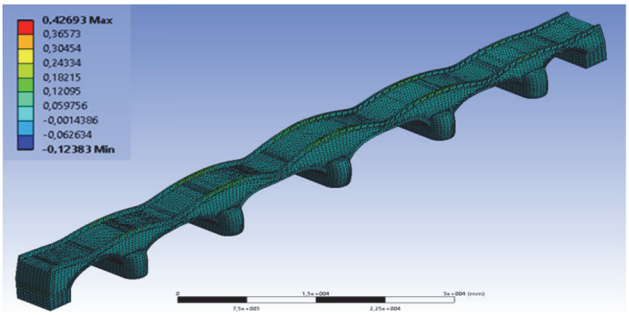

(a)

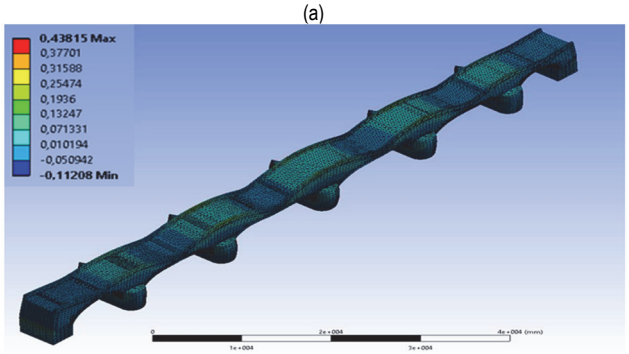

(b)

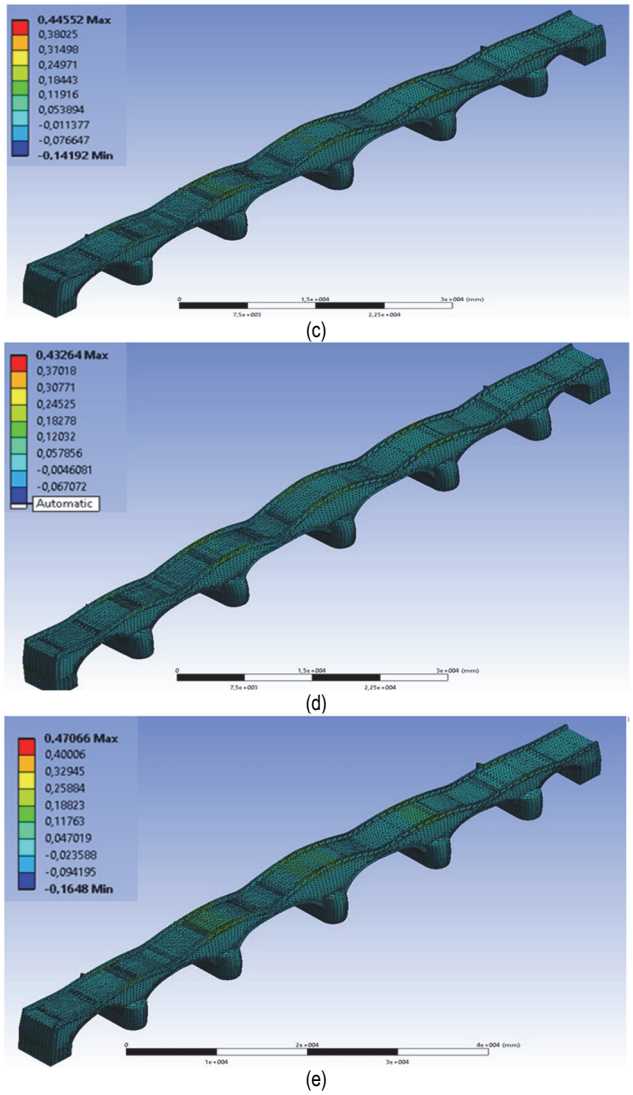

Figure 8 HAB max. principal stresses under far fault earthquakes: (a) EQ. #1; (b) EQ. #2; (c) EQ. #3; (d) EQ. #4; (e) EQ. #5

Table 4 Dynamic Analyses Consequences

Number #	Fault Form	EQ	Konjic Bridge		
			Deformation	Max. Principal Elastic Strain	Max. Principal Stress
			mm	mm/mm	MPa
1	Far Fault	Borrego Mount, 1968	1.24	0.00016	0.43
2		Friuli, Italy, 1976	1.39	0.00016	0.44
3		Kobe, 1995	1.29	0.00017	0.45
4		Morgan Hill, 1984	1.39	0.00018	0.47
5		NW California, 1941	1.24	0.00016	0.43

6 LIFE-CYCLE ASSESSMENT FOR KONJIC BRIDGE

Disruption might be produced as a consequence of loads and environmental properties. Though the deterioration rate is assumed to be good for concrete and steel bridges, there is fewer data for HABs in the literature. In this point, it is explored to decline models for HABs exactly as a consequence of predication. Though there are several methods considered for MAB in the literature, for instance Harvey [46], Gilbert and Melbourne [47], Fanning and Boothby [48], these are established on the static examination records and the properties of long-standing worsening as a consequence of traffic prediction and environmental properties are not considered. To take these features into account, Sustainable Masonry Arch Resistance Technique (SMART) is suggested [49]. Consuming that method, it is combined longtime service capacity and restrictions into the calculation. This method brings together all the present approaches into a particular method, in view of not only the ultimate load capability but also the longtime conduct and remaining life cycle for HABs [50]. In mathematical correlation, SN method offered for masonry by Roberts et al. established on a series of small-scale experiment site assessments [51]. According to experiment consequences, a stochastic model was established for MABs as presented in Eq. (1) by Casas [52];

$$S = A \cdot N^{-B(1-R)} > 0.5 \tag{1}$$

where, S is described as $S = S_{Max}/S_{Av}$. S_{Max} is described as percentage of the max. stress and S_{Av} is described as the average strength. Furthermore, N is described as the number of cycles and R is described as the proportion of the min. stress to the max. stress ($R = S_{Min}/S_{Max}$). A durability edge of 50% was expected. To form the useful presentation of SN curvatures, samples for stress stages and related lifecycle possibility are offered in Tab. 5 [52], according to Casas' model.

Table 5 Instances of estimated life expectation according to Casas [52]

Compression			Shear		
Stress	Average Life		Stress	Average Life	
%	Cycles	Ratio	%	Cycles	Ratio
45	8×10^9	35	45	1×10^8	18
50	2×10^8	1	50	7×10^6	1
55	1×10^7	1/20	55	6×10^5	1/12

Additionally, Tomor obtained the static test results and presented them as determined in Fig. 9 [50].

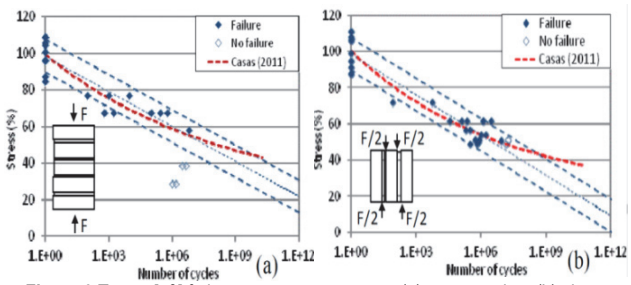

Figure 9 Tomor [50] fatigue test consequences: (a) compression; (b) shear

The value of B is established to 0.04 for the current test data [53]. While Fig. 9 is detected for compression, the life cycle expectation calculated for an average 50% stress grade is nearby 2×10^8 cycles. If this grade is decreased about 5% (from 50% to 45%), the life cycle expectation rises 35 times (from 2×10^8 to 8×10^9). On the other hand, if this grade is improved 5% (from 50% to 55%), the life cycle expectation decreases to around 1/20 (from 2×10^8 to 1×10^7). As stated above, while lifecycle calculation is imposed on the KB under different FFEs, it is detected that

stress values are improved from 0.41 to 0.47. Though it is detected that the stress showing tensile value has not touched the allowable sandstone TS and stress values appear to be so small, it is detected that historical MAB life is decreased significantly as a consequence of the amount of improvement in the TS (25%). As a consequence of this investigation, it is observed that though stress/strain values improve in small amounts as a consequence of FFEs, significant decreases in fatigue life occur. Consequently, Damage progress might take place over an extended date of time (even under comparatively low stress/strain stages).

7 CONCLUSIONS

In this research, a feature examination around the evaluation of static and dynamic productivity of a HAB in view of dissimilar FFEs is offered. Thus, F-E-M of the KB is made and investigated under numerous FFEs by the ANSYS. According to the analyses consequences, it is investigated that under the FFEs, TS have not touched the allowable masonry TS, specifically on the higher edge of the large archway, on the higher edge of the archway and pose hazard for destruction. It was observed that the compressive stresses are below the masonry compressive strength and are not imagined to be hazardous in the way of destruction. Additionally, for the KB, the possible destruction as a result of displacements is not established to be dangerous. Though, there is not displacement at the grade that would cause damage to the left behind parts of the KB. Additionally, observing these stress/strain values, life cycle assessment for HAB under these ground motions is also explored and observed that growing the longtime stress/strain values for HAB may decrease the HAB life-expectancy while stress/strain values have not reached the permissible masonry TS.

8 REFERENCES

[1] Dogangun, A. & Sezen, H. (2012). Seismic vulnerability and preservation of historical masonry monumental structures. *Earthquakes and Structures*, *3*(1), 83-95. https://doi.org/10.12989/EAS.2012.3.1.083

[2] Cakir, F. & Seker, B. S. (2015). Structural performance of renovated masonry low bridge in Amasya, Turkey. *Earthquakes and Structures*, *8*(6), 1387-1406. https://doi.org/10.12989/EAS.2015.8.6.1387

[3] Cakir, F., Ergen, Y. B., Uysal, H., & Dogangun, A. (2016). Influence of modified intended use on the seismic behavior of historical himis structures. *Earthquakes and Structures*, *10*(4), 893-911. https://doi.org/10.12989/EAS.2016.10.4.893

[4] Muvafik, M. (2014). Field investigation and seismic analysis of a historical brick masonry minaret damaged during the Van Earthquakes in 2011. *Earthquakes and Structures*, *6*(5), 457-472. https://doi.org/10.12989/EAS.2014.6.5.457

[5] Sayin, E. (2016). Nonlinear seismic response of a masonry arch bridge. *Earthquakes and Structures*, *10*(2), 483-494. https://doi.org/10.12989/EAS.2016.10.2.483

[6] Güllü, H. & Karabekmez, M. (2016). Gaziantep Kurtuluş Camisinin Deprem Davranışının İncelenmesi. *DÜMF Mühendislik Dergisi*, *7*(3), 455-470.

[7] Arnold, C. & Reitherman, R. (1982). *Building configuration and seismic design*. Wiley, New York.

[8] Kramer, S. L. (1996). *Geotechnical Earthquake Engineering*. Prentice Hall, New Jersey.

[9] Ural, A., Oruç, S., Doğangün, A., & Tuluk, Ö. İ. (2008). Turkish historical arch bridges and their deteriorations and failures. *Engineering Failure Analysis*, *15*, 43-53. https://doi.org/10.1016/j.engfailanal.2007.01.006

[10] Raychowdhury, P. (2009). Effect of soil parameter uncertainty on seismic demand of low-rise steel buildings on dense silty sand. *Soil Dynamics and Earthquake Engineering*, *29*, 1367-1378. https://doi.org/10.1016/j.soildyn.2009.03.004

[11] Luco, J. E. & Lanzi, A. (2013).Approximate soil-structure interaction analysis by a perturbation approach: the case of stiff soils. *Soil Dynamics and Earthquake Engineering*, *51*, 97-110. https://doi.org/10.1016/j.soildyn.2013.04.005

[12] Emre, Ö., Duman, T. Y., Olgun, S., Elmacı, H., & Özalp, S. (2012). *Active fault map of Turkey. Ankara (Turkey).* General Directorate of Mineral Research and Exploration.

[13] Preciado, A., Bartoli, G., & Budelmann, H. (2015). Fundamental aspects on the seismic vulnerability of ancient masonry towers and retrofitting techniques. *Earthquakes and Structures*, *9*(2), 339-352. https://doi.org/10.12989/EAS.2015.9.2.339

[14] Rovithis, E. N. & Pitilakis, K. D. (2016). Seismic assessment and retrofitting measures of a historic stone masonry bridge.*Earthquakes and Structures*, *10*(3), 645-667. https://doi.org/10.12989/EAS.2016.10.3.645

[15] Basaran, H., Demir, A., Ercan, E., Nohutcu, H., Hokelekli, E., & Kozanoglu, C. (2016). Investigation of seismic safety of a masonry minaret using its dynamic characteristics. *Earthquakes and Structures*, *10*(3), 523-538. https://doi.org/10.12989/EAS.2016.10.3.523

[16] Mazza, F. & Labernarda, R. (2017). Structural and non-structural intensity measures for the assessment of base-isolated structures subjected to pulse-like near-fau-lt earthquakes. *Soil Dynamics and Earthquake Engineering*, *96*, 115-27. https://doi.org/10.1016/j.soildyn.2017.02.013

[17] Breccolotti, M., Severini, L., Cavalagli, N., Bonfigli, F. M., & Gusella, V. (2018). Rapid evaluation of in-plane seismic capacity of masonry arch bridges through limit analysis. *Earthquakes and Structures*, *15*(5), 541-553. https://doi.org/10.12989/EAS.2018.15.5.541

[18] Pela, L., Aprıle, A., & Benedettı, A. (2009). Seismic Assessment of Masonry Arch Bridges. *Engineering Structures*, *31*, 1777-1788. https://doi.org/10.1016/j.engstruct.2009.02.012

[19] Page, J. (1993). *Masonry Arch Bridges - A State of the Art Review*. HMSO, London.

[20] Armstrong, D. M., Sibbald A., Fairfield C. A., & Forde M. C. (1995). Modal analysis for masonry arch bridge spandrel wall separation identification. *NDT& E International*, *28*(6), 377-386. https://doi.org/10.1016/0963-8695(95)00048-8

[21] Bensalem, A., Fairfield, C. A., & Sibbald, A. (1997). Non-destructive evaluation of the dynamic response of a brickwork arch. *ICE Journal of Structures and Buildings*, *122*(1), 69-82. https://doi.org/10.1016/S0963-695(98)00054-1

[22] Bensalem, A., Fairfield, C. A., & Sibbald, A. (1998). Damping effects on the NDT of soil backfilled arch bridges. *Journal of British Institute NDT*, *40*(2), 107-116.

[23] Karalar, M. & Yeşil, M. (2021). Investigation on Seismic Behavior of Historical Tokatlı Bridge under Near-Fault Earthquakes. *Advances in Civil Engineering*, *2021*, 18. https://doi.org/10.1155/2021/5596760

[24] Sigmund, Z., Radujković, M., & Lazarević, D. (2016). Decision support model for seismic strengthening technology selection of masonry buildings. *Tehnički vjesnik*, *23*(3), 791-800. https://doi.org/10.17559/TV-20151208142529

[25] Bošnjak-Klečina, M. & Lozančić, S. (2010).Testing of Physical and Mechanical Properties of Bricks and Mortar in Historic Structures. *Tehnicki Vjesnik - Technical Gazette*, *17*, 209-215.

[26] Sayın, E., Karaton, M., & Calayır, Y. (2016).Nonlinear seismic analysis of historical Topuzlu Dam under different seismic loads. *Građevinar*, *68*(11), 919-925. https://doi.org/10.14256/JCE.1595.2016
[27] Karalar, M. & Yeşil, M. (2021). Effect of near-fault earthquakes on a historical masonry arch bridge (Konjic Bridge). *Earthquakes and Structures*, *21*(2), 125-136. https://doi.org/10.12989/eas.2021.21.2.125
[28] Özmen, A. & Sayın, E. (2023). 3D Soil Structure Interaction Effects on the Seismic Behavior of Single Span Historical Masonry Bridge. *Geotechnical and Geological Engineering*. https://doi.org/10.1007/s10706-023-02389-6
[29] Hatzigeorgiou, G. D., Beskos, D. E., Teodorakopoulos, D. D., & Sfakianaki, M. (1999). Static and dynamic analysis of the Arta Bridge by finite elements. *Archives of Civil and Mechanical Engineering*, *2*(1), 41.
[30] Fanning, P. J. & Boothby, T. E. (2001). Three-dimensional modelling and full-scale testing of stone arch bridges. *Computers and Structures*, *79*(29), 2645-2662. https://doi.org/10.1016/S0045-7949(01)00109-2
[31] Frunzio, G., Monaco, M., & Gesualdo, A. (2001). 3D F.E.M. analysis of a Roman arch bridge. *Historical Constructions*, 591-598.
[32] Ünay, A. İ. & Toker, S. (2004). Mathematical Modeling and Finite Element Analysis of Masonry Arch Bridges. *Gazi University Journal of Science*, *17*(2), 127-137.
[33] Ural A. (2005). Finite element analysis of historical arch bridge. *International Earthquake Symposium Kocaeli*, *23*, 408-413.
[34] Bayraktar, A., Altunısık, A. C, Turker, T., & Sevim, B. (2007). The model updating of historical masonry bridges using operational modal analysis method. *Proceedings of the 1st National Conference Reinforcement and Transfer into the Future of Historical Structures*, 429-440.
[35] Brencich, A. & Sabia, D. (2008). Experimental identification of a multi-span masonry bridge: The Tanaro Bridge. *Construction and Building Materials*, *22*, 2087-2099. https://doi.org/10.1016/j.conbuildmat.2007.07.031
[36] Diamanti, N., Giannopoulos, A., & Forde, M. C. (2008). Numerical modelling and experimental verification of GPR to investigate ring separation in brick masonry arch bridges. *NDT and E International*, *41*(5), 354-363. https://doi.org/10.1016/j.ndteint.2008.01.006
[37] Aydin, A. C. & Ozkaya, S. G. (2018). The finite element analysis of collapse loads of single-spanned historic masonry arch bridges (Ordu, Sarpdere Bridge). *Engineering Failure Analysis*, *84*, 131-138. https://doi.org/10.1016/j.engfailanal.2017.11.002
[38] Bouzas, O. Conde, B., Matos, J. C., Solla, M., & Cabaleiro, M. (2023). Reliability-based structural assessment of historical masonry arch bridges: The case study of Cernadelabridge. *Case Studies in Construction Materials*, *18*. https://doi.org/10.1016/j.cscm.2023.e02003
[39] Alpaslan, E., Yilmaz, M. F., & Dinç Şengönül, B. (2023). Rating and reliability assessment of a historical masonry arch bridge. *Journal of Civil Structural Health Monitoring*, *1*(1), 1-19. https://doi.org/10.1007/s13349-023-00692-7
[40] Sert, H., Partal, E., Demirci, H., Avşin, A., & Yılmaz S. (2009). Tarihi Köprüler Projeve Uygulama İhaleleri. *Karayolları Genel Müdürlüğü Yayınları*, 54.
[41] ANSYS. ANSYS Inc., Canonsburg, Pensnsylvania, (1998).
[42] Kamil, J. A. Khan, I. A., & Nath, Y. (2011). Numerical and Experimental Dynamic Contact of Rotating Spur Gear. *Modern Applied Science*, *5*, 254-263.
[43] Kadhim, M. M. A. (2012). Factors effect on the effective length in a double strap joint between steel plates and CFRP. *International Journal of Advances in Applied Sciences*, *1*, 11-18.
[44] Makris, N. & Black, J. C. (2004). Evaluation of peak ground velocity as a "Good" intensity measure for near-source ground motions. *Journal of Engineering Mechanics*, *130*(9), 1032-1044.
[45] Makris, N. & Chang, S. (1998). *Effect of damping mechanisms on the response of seismically isolated structures*. PEER-98/06, Pacific Earthquake Engineering Research Center, Berkeley, CA,
[46] Harvey, W. (1988). Application of the mechanism analysis to masonry arches. *The Structural Engineer*, *66*(5), 77-84.
[47] Gilbert, M. & Melbourne, C. (1994). Rigid-block analysis of masonry structures. *Structural Engineering*, *72*(21), 356-361.
[48] Fanning, P. & Boothby, T. (2001). Three-dimensional modelling and full-scale testing of stone arch bridges. *Computers and Structures*, *79*(29-30), 2645-2662. https://doi.org/10.1016/S0045-7949(01)00109-2
[49] Melbourne, C., Wang, J., & Timor, A. (2007). A New Masonry Arch Bridge Assessment Method (SMART). *Proceedings of the Institution of Civil Engineering - Bridge Engineering*, *160*(2). 81-87.
[50] Tomor, A. (2013). Life-cycle assessment and deterioration models for masonry arch bridges. *WIT Transactions on Ecology and the Environment*, *179*, 535-546.
[51] Roberts, T., Hughes, T., Dandamudi, V., & Bell, B. (2006). Quasi-static and high cycle fatigue strength of brick masonry. *Construction and Building Materials*, *20*(9), 603-614. https://doi.org/10.1016/j.conbuildmat.2005.02.013
[52] Casas, J. R. (2011). Reliability-based assessment of masonry arch bridges. *Construction and Building Materials*, *25*(4), 1621-31. https://doi.org/10.1016/j.conbuildmat.2010.10.011
[53] Tomor, A. & Verstrynge, E. (2013).A joint fatigue–creep deterioration model for masonry with acoustic emission based damage assessment. *Construction and building Materials*, *43*, 575-588. https://doi.org/10.1016/j.conbuildmat.2013.02.045
[54] Sevim, B., Bayraktar, A., Altunışık, A. C., Atamtürktür, S., & Birinci, F. (2011). Assessment of nonlinear seismic performance of a restored historical arch bridge using ambient vibrations. *Nonlinear Dynamics*, *63*, 755-770. https://doi.org/10.1007/s11071-010-9835-y
[55] Şeker, S. & Şahin, H. (2022).Evaluation of the seismic behavior of the historic Clandrasbridge. *Usak University Journal of Engineering Sciences*, *5*(1), 1-12. https://doi.org/10.47137/uujes.1055725
[56] Batar, O. S., Tercan, E., & Emsen, E. (2021). Ayvalıkemer (Sillyon) historical masonry arch bridge: a multidisciplinary approach for structural assessment using point cloud data obtained by terrestrial laser scanning (TLS). *Journal of Civil Structural Health Monitoring*, *11*, 1239-1252. https://doi.org/10.1007/s13349-021-00507-7

Contact information:

Memduh KARALAR
(Corresponding author)
Zonguldak Bulent Ecevit University,
Department of Civil Engineering
E-mail: memduhkaralar@beun.edu.tr

Mustafa YEŞİL
Zonguldak Bulent Ecevit University,
Department of Civil Engineering
E-mail: Mustafa.yesil@windows.live.com